Published in final edited form as:
J Am Coll Cardiol. 2007 June 12; 49(23): 2292–2300. doi:10.1016/j.jacc.2007.02.050.

An Elastic, Biodegradable Cardiac Patch Induces Contractile Smooth Muscle and Improves Cardiac Remodeling and Function in Subacute Myocardial Infarction

Kazuro L. Fujimoto, MD[*,†], **Kimimasa Tobita, MD**[†,‡,§], **W. David Merryman, PhD**[§], **Jianjun Guan, PhD**[*,†], **Nobuo Momoi, MD, PhD**[‡], **Donna B. Stolz, PhD**[‖], **Michael S. Sacks, PhD**[†,§], **Bradley B. Keller, MD**[†,‡,‖], and **William R. Wagner, PhD**[*,†,§]

[*]Department of Surgery, Children's Hospital of Pittsburgh, Pittsburgh, Pennsylvania

[†]McGowan Institute for Regenerative Medicine, Pittsburgh, Pennsylvania

[‡]Department of Pediatrics, Children's Hospital of Pittsburgh, Pittsburgh, Pennsylvania

[§]Department of Bioengineering, University of Pittsburgh, Pittsburgh, Pennsylvania

[‖]Department of Cell Biology and Physiology, University of Pittsburgh, Pittsburgh, Pennsylvania

Abstract

Objectives—Our objective in this study was to apply an elastic, biodegradable polyester urethane urea (PEUU) cardiac patch onto subacute infarcts and to examine the resulting cardiac ventricular remodeling and performance.

Background—Myocardial infarction induces loss of contractile mass and scar formation resulting in adverse left ventricular (LV) remodeling and subsequent severe dysfunction.

Methods—Lewis rats underwent proximal left coronary ligation. Two weeks after coronary ligation, a 6-mm diameter microporous PEUU patch was implanted directly on the infarcted LV wall surface (PEUU patch group, n = 14). Sham surgery was performed as an infarction control (n = 12). The LV contractile function, regional myocardial wall compliance, and tissue histology were assessed 8 weeks after patch implantation.

Results—The end-diastolic LV cavity area (EDA) did not change, and the fractional area change (FAC) increased in the PEUU patch group ($p < 0.05$ vs. week 0), while EDA increased and FAC decreased in the infarction control group ($p < 0.05$). The PEUU patch was largely resorbed 8 weeks after implantation and the LV wall was thicker than infarction control ($p < 0.05$ vs. control group). Abundant smooth muscle bundles with mature contractile phenotype were found in the infarcted myocardium of the PEUU group. The myocardial compliance of the PEUU group was distributed between normal myocardium and infarction control ($p < 0.001$).

Conclusions—Implantation of a novel biodegradable PEUU patch onto a subacute myocardial infarction promoted contractile phenotype smooth muscle tissue formation and improved cardiac remodeling and contractile function at the chronic stage. Our findings suggest a new therapeutic option against post-infarct cardiac failure.

Postinfarct left ventricular (LV) remodeling is a well-described compensatory mechanism of congestive heart failure (CHF), characterized by progressive ventricular chamber dilatation,

Reprint requests and correspondence: Dr. William R. Wagner, McGowan Institute for Regenerative Medicine, University of Pittsburgh, 100 Technology Drive, Pittsburgh, Pennsylvania 15219. wagnerwr@upmc.edu.

wall thinning, and sphericity that allows the failing ventricle to maintain cardiac output by increasing stroke volume. This compensatory mechanism in the long-term causes maladaptive changes in myocardial structural and function (1,2). Among clinical indicators, LV dilation and increased LV sphericity are sensitive predictors of poor long-term outcome and mortality (3). Therapeutic strategies to antagonize LV remodeling, such as angiotensin-converting enzyme inhibitors and/or beta-blockers, have proven beneficial in treating CHF (4). Despite the value of such medical approaches, progression from myocardial infarction to CHF remains a tremendous burden in terms of morbidity and mortality as well as financial cost.

Surgical approaches have been proposed that are based on the concept of reducing the LV cavity volume to restore wall tension toward normal levels, thus interrupting the remodeling process and improving hemodynamic status. Both the endoventricular circular patch plasty technique (the Dor procedure) (5,6) and partial left ventriculectomy (the Batista procedure) (7) have been clinically implemented. However, these therapies are restricted to patients with severe dilation and dysfunction many years after an infarction. Another surgical approach that has been investigated is epicardial restraint therapy, where a wrap is applied over the cardiac surface from the apex upward. The Acorn Cardiac Support Device (Acorn Cardiovascular, St. Paul, Minnesota), which is comprised of a polyester mesh (8), and the Paracor device (Paracor Medical, Inc., Sunnyvale, California), which utilizes a nitinol mesh (9), employ this strategy. These approaches both utilize nonbiodegradable materials and result in a permanent foreign body encapsulating the epicardium. More recently, several groups have pursued tissue engineering approaches for ventricular wall reconstruction surgery (10-12), in contrast to the wide variety of cellular injection approaches currently under investigation (13). The feasibility of translating these latter approaches to the clinic remains challenging with concerns about cell sourcing and characterization, and the practicalities of in vitro patch development being of concern.

Given these observations, we hypothesized that an attractive approach to the management of LV dilation would be to apply an elastic patch to the infarcted ventricle where the patch was not a wrap, but might be sized to the infarct, and where the patch was both highly elastic and biodegradable so that the material would erode over several weeks. By avoiding cellular components, the approach might be more readily translatable to clinical investigations. Toward this end, we have designed and developed a porous, elastic scaffold from a biodegradable elastomer that can be processed into a variety of formats compatible with cardiovascular placement (14,15). Our objective in this study was to apply this scaffold as a cardiac patch onto subacute infarcts that had developed over a 2-week period after coronary ligation in the rat model and to examine the resulting cardiac performance and ventricular remodeling. Our hypothesis was that placement of this patch would alter the progression of remodeling, which leads to ventricular wall thinning and fibrosis, and would preserve contractile function.

Methods

Experimental animals

Adult female Lewis rats (Harlan Sprague Dawley, Indianapolis, Indiana) weighing 200 g to 250 g were used. The protocol followed National Institutes of Health guidelines for animal care and was approved by the University of Pittsburgh's Institutional Animal Care and Use Committee and Children's Hospital of Pittsburgh Animal Research Care Committee.

Elastomeric biodegradable microporous polyester urethane urea (PEUU) patch

The circular PEUU patch was made of a polyester urethane urea that was synthesized in the investigators' laboratory as previously described (14), and processed using thermally induced phase separation techniques (15) into a patch with interconnected micropores (Fig. 1A). The patch possessed 91% porosity and a 91-μm average pore size. Mechanically, the patch was elastic with a tensile strength of 0.78 MPa and elongation at rupture of 157%. The material was sized to circular patches 6 mm in diameter × 300 μm thick (Fig. 1B). The patches were immersed in 100% ethanol for 30 min, followed by immersion in phosphate-buffered saline and exposure to the ultraviolet light source for 1 h before implantation.

Proximal left coronary artery ligation

Animal anesthesia was induced by 3.0% isoflurane inhalation followed by intubation and connection to a rodent volume-controlled mechanical ventilator. The heart was exposed through a left thoracotomy, monitoring electrocardiogram, and tail cuff blood pressure. The proximal left anterior descending coronary artery was ligated with 7-0 polypropylene. Myocardial ischemia was confirmed by regional cyanosis and ST-segment elevation. The incision was closed in layers with 4-0 silk continuous sutures.

PEUU patch implantation

Two weeks after coronary artery ligation, animals were anesthetized and examined echocardiographically for infarct size as estimated by the percentage of scar area (akinetic or dyskinetic regions) to LV free wall area (11). A total of 26 rats with infarcts greater than 25% of the LV free wall were divided into 2 groups: PEUU patch repair (patch group; n = 14) and sham repair (infarction control group; n = 12). Through a left thoracotomy, the infarcted anterior wall was exposed. Before affixing the patch, the surface of the infarcted area (less than 0.1 mm thickness), including the remnant epicardium and some of the integrated fibrous tissue, was scraped and removed at the patch implant site. Using 7-0 polypropylene with over-and-over peripheral sutures, the anterior infarcted myocardium was covered with a PEUU patch. For the infarction control group, a thoracotomy was performed 2 weeks after coronary ligation, but no scraping or patch placement was performed. Six age-matched rats without coronary ligation or surgical intervention served as a control group.

Histology

Eight weeks after patch implantation (10 weeks after myocardial infarction), rats in both surgical groups were anesthetized, and the heart was exposed and arrested by apical injection of 2 ml of a hypothermic arresting solution (68 mmol/l NaCl, 60 mmol/l KCl, 36 mmol/l $NaHCO_3$, 2.0 mmol/l $MgCl_2$, 1.4 mmol/l Na_2SO_4, 11 mmol/l dextrose, 30 mmol/l butanedione monoxime, 10,000 U/l of heparin). The embedded frozen LV tissues were serially sectioned at 8 μm in the LV transverse direction. Hematoxylin and eosin staining and immunohistochemical staining were performed as previously described (16) with antibodies against alpha-smooth muscle actin (SMA) (Sigma, St. Louis, Missouri), CD 31 (Serotec, Raleigh, North Carolina), caldesmon (Abcam, Cambridge, Massachusetts), calponin (Abcam), smooth muscle myosin heavy chain 2 (SMMHC-2, Abcam), SM-22α (Abcam), basic fibroblast growth factor (bFGF, Serotec), or vascular endothelial growth factor (VEGF, Santa Cruz Biotechnology, Santa Cruz, California). Nuclei were stained with 4′,6-Diamidino-2-phenyindole (DAPI, Sigma). To observe the pattern of α-SMA–positive staining across the infarcted wall, 5 to 7 fields at 100× were digitally photographed for each heart and composite images assembled (NIH image and Adobe Photoshop, San Jose, California) (n = 5 rats/group).

LV wall thickness and capillary density

For each LV sample, 5 different microscopic fields at 100× for the wall thickness measurement and 10 different fields at 200× for capillary density were photographed for each rat. The wall thickness of the infarcted anterior wall (patch implanted region) was analyzed using NIH Image software for patch and infarction control groups (n = 5 rats/group). Capillaries were recognized as tubular structures positively stained for CD31 as previously described (16).

Transmission electron microscopy

Two hearts from each group were processed and imaged with transmission electron microscopy as previously described (17). Thin sections (80 nm) were examined with JEOL 1210 TEM system (JEOL USA, Peabody, Massachusetts). Digital images were obtained using a side-mount AMT 2k digital camera (Advanced Microscopy Technologies, Danvers, Massachusetts).

Echocardiography

Echocardiography was performed at the time of patch implantation (0 weeks, 2 weeks postinfarction), 4 and 8 weeks after patch implantation. The same time points were measured for all groups. Rats were anesthetized with isoflurane inhalation. Standard transthoracic echocardiography was performed using the Acuson Sequoia C256 system with 13-MHz linear ultrasonic transducer (15L8; Acuson Corporation, Mountain View, California) in a phased-array format. B-mode measurements on the LV short-axis view (papillary muscle level) were performed (16). The end-diastolic (EDA) and end-systolic (ESA) LV internal cavity areas were measured by tracing the endocardial border. The regional EDA and ESA at the infarcted antero-lateral wall segment were also measured using a floating centroid method (18). The global and regional LV fractional area change (%FAC) were estimated as $\%FAC = [(LVEDA - LVESA) \div LVEDA] \times 100\%$. All measurements were performed using Scion Image software (Scion Image, Fredrick, Maryland).

Regional myocardial compliance

Passive LV inflation was performed to quantify regional myocardial compliance in the infarction zone (19). Coronary circulation was perfused through an aortic cannula with arresting solution. After perfusion, coronary arteries were occluded at the coronary ostium, and mitral leaflets were completely closed by 7-0 polypropylene suture. For LV surface strain measurements, 4 small graphite particles were placed 4 mm apart in a square configuration on the center of infarcted LV epicardial surface with butyl-cyanoacrylate glue. The heart was submerged in a chamber containing arresting solution that allowed entrance of a boroscope coupled to a CCD camera for imaging. As the infarcted region was sufficiently small (6-mm diameter), dual-camera, stereo imaging of the curved surface was unnecessary. Markers were tracked continuously using a customized LabVIEW (National Instruments, Austin, Texas) program.

Ventricular pressure was applied with a volume-infusion pump (model sp210w, World Precision Instruments, Sarasota, Florida) that formed a continuous connection with the lured cannula and a 2-F micromanometer-tipped catheter (model SPR631, Millar Instruments, Houston, Texas). During infusion, real-time strains in both directions (circumferential, E_{11} and longitudinal, E_{22}) were computed from 2-dimensional marker displacements using previous methods (20), and the applied pressure was simultaneously recorded. The inflation test was performed sequentially 3 times in each sample by infusing arresting solution to a maximum pressure of 30 mm Hg, confirming that inflation/deflation volumes were

reproducible for all cycles. Pressure-strain (P-E) relations were determined for all groups (n = 4 rats/group).

Statistics

All data are expressed as mean ± standard deviation. Analyses utilized SPSS software (SPSS Inc., Chicago, Illinois). The wall thickness in each group was compared by Student *t* test. Echocardiography data and P-E analyses were compared by 2-way repeated analysis of variance with Tukey's test. Statistical significance was defined at a value of $p < 0.05$.

Results

External morphology

There were no early or late postoperative deaths in either surgical group. After an 8-week implantation period, the PEUU patch material was found to have formed no strong adhesions with the chest wall, and its surface was covered with connective tissue (Figs. 1C and 1F). In examining the heart in transverse cross section, it was consistently found that the patch was well merged with the cardiac tissue and restored the LV wall thickness in the infarction region relative to hearts from the infarction control group.

Histology

In examining histological sections stained with hematoxylin and eosin, it was seen that the majority of the PEUU patch was absorbed and the remnant area of the patch appeared to be infiltrated with macrophages and fibroblasts. The ventricular walls to which PEUU patches were applied were thicker and contained more dense and muscle-like bundles than the infarction control (Figs. 2A and 2B). The muscle-like bundles were found under the patch regions stained positively for α-SMA (Figs. 2C to 2F). Reviewing α-SMA expression across the infarct region from 5 random samples in each experimental group demonstrated that in the infarction control group, α-SMA was sporadically expressed and primarily associated with vascular structures in all samples. In contrast, for the PEUU patch group, there were 2 patterns of α-SMA staining: a uniform distribution of α-SMA–positive tissue beneath the whole patch area, or clustered regions of α-SMA–positive tissue. Further immunohistochemical staining demonstrated that caldesmon, calponin, SM 22α, and SMMHC-2 (Fig. 3A), proteins that are associated with contractile function, co-localized with α-SMA–positive cells. Electron micrographs of the muscle-like bundles demonstrated that the aligned cells were rich in myofibrils and clustered mitochondria typical of smooth muscle cell ultrastructure. Numerous caveolae along the membrane and dense bodies within the cytoplasm were observed, strongly suggesting a smooth muscle phenotype (Figs. 3B to 3D).

Wall thickness and capillary density

From histological section analysis, the LV myocardial wall for the PEUU implantation group was found to be thicker than that in the infarction control group (985 ± 90 μm vs. 480 ± 62 μm, $p < 0.01$). The capillary density of the PEUU patch group was significantly increased compared with that in the infarction control group ($275 \pm 56/mm^2$ vs. $102 \pm 17/mm^2$, $p < 0.05$).

Growth factor expression

Basic fibroblast growth factor and VEGF immunohistochemical staining (Figs. 4A to 4D) demonstrated expression of both growth factors around the capillaries and smooth muscle bundles in the PEUU patch group, whereas in the infarction control group, staining for both growth factors was sparse and appeared to be associated with vascular structures.

LV cavity size and contractile function

A significant interaction was found to exist between the experimental groups and observed time points ($p < 0.001$). At the time of PEUU patch implantation (0 weeks), the LV EDA was significantly larger, and the %FAC was significantly smaller than for the age-matched normal control animals, confirming post-infarction LV dilation and dysfunction. The patch group did not experience a change in EDA after patch implantation at any of the time points, while at 8 weeks, the EDA of the infarction control group was significantly increased versus the 0 week point (Fig. 5). The EDA of the infarction control group at 8 weeks was also significantly larger than that of the patch group. The %FAC was increased in the patch group at 8 weeks relative to the time of patch implantation, while for the infarction control group the %FAC had significantly decreased by 8 weeks. The regional %FAC in the PEUU patch group at 8 weeks was significantly larger than that in the infarction control group (27 ± 9.0% vs. 15 ± 10%), which was similar to the global %FAC. It was noted that negative values of %FAC (dyskinetic) were obtained for 2 samples of the infarction control group, an effect not observed in the PEUU patch group.

Regional LV myocardial compliance

Both circumferential and longitudinal LV myocardial P-E curves (Fig. 6) revealed that at 8 weeks the LV wall had stiffened in the infarction control group and exhibited the least compliance. Pressure-strain curves for the PEUU patch group fell between the normal and infarction groups in the circumferential direction ($p < 0.001$) and in the longitudinal direction followed essentially the same path as the normal group.

Discussion

Our results demonstrated that implantation of an elastic, biodegradable PEUU patch onto the ventricular region of a subacute myocardial infarct in the rat model preserved LV geometry and improved contractile function relative to that in nontreated animals. This effect occurred even though the patch was placed 2 weeks after the time of LV infarction. During this clinically relevant lag period preceding intervention, the infarcted wall would be expected to have progressed through the necrotic phase and into the fibrotic phase (2). A particularly encouraging finding was the effect that patch placement had on tissue remodeling at the structural level with the development of smooth muscle bundles in the tissue below the patch and the alteration in myocardial wall thickness and compliance.

The PEUU material was chosen for its elastic mechanical properties, processability, expected biocompatibility, and biodegradability (14,15). It was shown that after 8 weeks of implantation, most of the material had degraded in vivo. By utilizing an elastic, degradable patch material, it was postulated that temporary alteration of the mechanical environment would provide benefit, and that by degrading, the PEUU material would avoid potential complications associated with a nondegradable material such as providing a chronic nidus for infection and calcification. Also, our experience with the regional application was a 0% mortality rate with minimal adhesion formation evident at the time of explant as well as no evidence of infection. Should this approach be scalable to humans, one would expect that the procedure could be performed in a low-risk manner and the mechanical properties of the PEUU material also were amenable to rolling, folding, or other compression techniques that might allow the patch to be placed minimally invasively.

Several possible mechanisms might explain the functional benefits associated with the patch. First, mechanical reinforcement provided by the PEUU material would acutely act to prevent further LV dilatation, which subsequently increases LV wall tension (6). Second, increased wall thickness, even after the patch had degraded, might reduce LV wall stress

versus untreated infarct control. Finally, the regional myocardial compliance of patched myocardium approached that of normal myocardium and was significantly higher than infarction control, which stiffened. This near normal physiologic compliance might act to prevent further LV dilation and improve cardiac function. Our findings would appear to contradict the work of Pfeffer et al. (21) where it was reported that LV chamber compliance increases (by pressure-volume relations) after infarction. However, Omens et al. (22) demonstrated that the regional LV strain P-E response after infarction may not be well predicted by the overall LV chamber pressure-volume response. With respect to the abundant contractile smooth muscle cell bundles found in the LV walls of patched animals, there is no evidence that they contributed to LV function, and further studies would be necessary to examine this potential effect.

In considering the role of the inflammatory response associated with PEUU biodegradation, this phenomenon might act to enhance and extend the presence of granulation tissue in the infarct area, analogous to the effect pursued by Hayakawa et al. (23). The PEUU will degrade by hydrolysis and, when small enough particles are generated, be phagocytosed by macrophages at the implant site. We found pronounced expression of bFGF and VEGF around the vessels and smooth muscle bundles in the PEUU patch group with significantly increased capillary density relative to infarction control. These locally released angiogenic factors, potentially released by local macrophages, might positively influence tissue remodeling. In addition to material phagocytosis, the scraping procedure employed before patch placement might augment this local inflammatory response acutely. Further studies to define specific growth factor and cytokine release patterns would be warranted.

Several limitations of the current report should be mentioned. First, the beneficial effects in terms of cardiac function and LV remodeling were only observed in the 8-week period after patch implantation. Although the PEUU patch has substantially degraded in this period, the sustainability of the architectural and functional changes remains to be examined for longer periods of time. There might theoretically be some optimal time point when the patch would have provided its beneficial effect and degradation would be desired. To investigate this effect, the time course of patch degradation could be altered by manipulating the polymer chemistry while maintaining comparable mechanical properties (24). A second limitation of this report was employment of the rat model. Further exploration in a large animal model is needed where changes in the patched LV area and the volume of impacted LV wall more closely approximate the clinical setting. Finally, the origin of the smooth muscle cell bundles that appear in the patched LV wall has not been defined. Histological sections did not suggest an obvious migration of this tissue from the healthy periphery of the infarct. One hypothesis is that this tissue is derived from circulating cells rather than myocardial tissue. Employment of a marrow ablation model where a chimera with fluorescently labeled reconstituted marrow is obtained would permit investigation of this theory (25).

Conclusions

This report demonstrates that regional application of a biodegradable and elastic polyurethane cardiac patch prevented ventricular dilation and improved contractile function in a subacute rat infarction model. This approach might provide an attractive alternative to cellular cardiomyoplasty or larger ventricular restraint devices for cardiac repair.

Acknowledgments

The authors thank Jennifer Debarr, Katie Clark, Ana Lopez, Mara Sullivan, and Kenichi Tamama for their help with the tissue histological assessment, and Paul Bieniek for writing software code for biomechanical compliance measurements.

This work was supported by the National Heart, Lung, and Blood Institute, grant HL069368.

References

1. Mann DL, Bristow MR. Mechanisms and models in heart failure: the biomechanical model and beyond. Circulation 2005;111:2837–49. [PubMed: 15927992]
2. Holmes JW, Borg TK, Covell JW. Structure and mechanics of healing myocardial infarcts. Annu Rev Biomed Eng 2005;7:223–53. [PubMed: 16004571]
3. White HD, Norris RM, Brown MA, Brandt PW, Whitlock PM, Wild CJ. Left ventricular end-systolic volume as the major predictor of survival after recovery from myocardial infarction. Circulation 1987;76:44–51. [PubMed: 3594774]
4. Sabbah HN, Shimoyama H, Kono T, et al. Effects of long-term monotherapy with enalapril, metoprolol, and digoxin on the progression of left ventricular dysfunction and dilation in dogs with reduced ejection fraction. Circulation 1994;89:2852–9. [PubMed: 8205701]
5. Dor V, Sabatier M, DiDonato M, Montiglio F, Toso A, Maioli M. Efficacy of endoventricular patch plasty in large postinfarction akinetic scar and severe left ventricular dysfunction: comparison with a series of large dyskinetic scars. J Thorac Cardiovasc Surg 1998;116:50–9. [PubMed: 9671897]
6. Kawaguchi AT, Suma H, Konertz W, et al. International and Regional Registry Task Force, the Society for Cardiac Volume Reduction. Left ventricular volume reduction surgery: the 4th International Registry Report 2004. J Card Surg 2005;20:S5–11. [PubMed: 16305637]
7. Batista RJ, Verde J, Nery P, et al. Partial left ventriculectomy to treat end-stage heart disease. Ann Thorac Surg 1997;64:634–8. [PubMed: 9307450]
8. Chaudhry PA, Mishima T, Sharov VG, et al. Passive epicardial containment prevents ventricular remodeling in heart failure. Ann Thorac Surg 2000;70:1275–80. [PubMed: 11081885]
9. Magovern JA. Experimental and clinical studies with the Paracor cardiac restraint device. Semin Thorac Cardiovasc Surg 2005;17:364–8. [PubMed: 16428045]
10. Leor J, Aboulafia-Etzion S, Dar A, et al. Bioengineered cardiac grafts: a new approach to repair the infarcted myocardium? Circulation 2000;102:56–61.
11. Matsubayashi K, Fedak PW, Mickle DA, Weisel RD, Ozawa T, Li RK. Improved left ventricular aneurysm repair with bioengineered vascular smooth muscle grafts. Circulation 2003;108:219–25.
12. Kellar RS, Shepherd BR, Larson DF, Naughton GK, William SK. Cardiac patch constructed from human fibroblasts attenuates reduction in cardiac function after acute infarct. Tissue Eng 2005;11:1678–87. [PubMed: 16411813]
13. Welt FG, Losordo DW. Cell therapy for acute myocardial infarction: curb your enthusiasm? Circulation 2006;113:1272–4. [PubMed: 16534025]
14. Guan J, Sacks MS, Beckman EJ, Wagner WR. Synthesis, characterization, and cytocompatibility of elastomeric, biodegradable poly(ester-urethane) ureas based on poly(caprolactone) and putrescine. J Biomed Mater Res 2002;61:493–503. [PubMed: 12115475]
15. Guan J, Fujimto KL, Sacks MS, Wagner WR. Preparation and characterization of highly porous, biodegradable polyurethane scaffolds for soft tissue applications. Biomaterials 2005;26:3961–71. [PubMed: 15626443]
16. Oshima H, Payne TR, Urish KL, et al. Differential myocardial infarct repair with muscle stem cells compared to myoblasts. Mol Ther 2005;12:1130–41. [PubMed: 16125468]
17. Michalopoulos GK, Bowen WC, Zajac VF, et al. Morphogenetic events in mixed cultures of rat hepatocytes and nonparenchymal cells maintained in biological matrices in the presence of hepatocyte growth factor and epidermal growth factor. Hepatology 1999;29:90–100. [PubMed: 9862855]
18. Carstensen S, Hoest U, Kjoeller-Hansen L, Saunamaki K, Atar D, Kelbaek H. Comparison of methods of fractional area change for detection of regional left ventricular dysfunction. Int J Card Imaging 2000;16:257–66. [PubMed: 11219597]
19. Emery JL, Omens JH, McCulloch AD. Biaxial mechanics of the passively overstretched left ventricle. Am J Physiol 1997;272:2299–305.
20. Sacks MS. Biaxial mechanical evaluation of planar biological materials. J Elast 2000;61:199–246.

21. Pfeffer JM, Pfeffer MA, Fletcher PJ, Braunwald E. Progressive ventricular remodeling in rat with myocardial infarction. Am J Physiol 1991;260:H1406–14. [PubMed: 2035662]
22. Omens JH, Miller TR, Covell JW. Relationship between passive tissue strain and collagen uncoiling during healing of infarcted myocardium. Cardiovasc Res 1997;33:351–8. [PubMed: 9074699]
23. Hayakawa K, Takemura G, Kanoh M, et al. Inhibition of granulation tissue cell apoptosis during the subacute stage of myocardial infarction improves cardiac remodeling and dysfunction at the chronic stage. Circulation 2003;108:104–9. [PubMed: 12821555]
24. Guan J, Sacks MS, Beckman EJ, Wagner WR. Biodegradable poly-(ether ester urethane) urea elastomers based on poly(ether ester) triblock copolymers and putrescine: synthesis, characterization and cytocompatibility. Biomaterials 2004;25:85–96. [PubMed: 14580912]
25. Toyokawa H, Nakao A, Stolz DB, et al. 3D-confocal structural analysis of bone marrow-derived renal tubular cells during renal ischemia/reperfusion injury. Lab Invest 2006;86:72–82. [PubMed: 16258520]

Abbreviations and Acronyms

bFGF	basic fibroblast growth factor
CHF	congestive heart failure
EDA	end-diastolic left ventricular cavity area
ESA	end-systolic left ventricular cavity area
FAC	fractional area change
LV	left ventricular
PEUU	polyester urethane urea
P-E	pressure-strain
SMA	smooth muscle actin
SMMHC-2	smooth muscle myosin heavy chain 2
VEGF	vascular endothelial growth factor

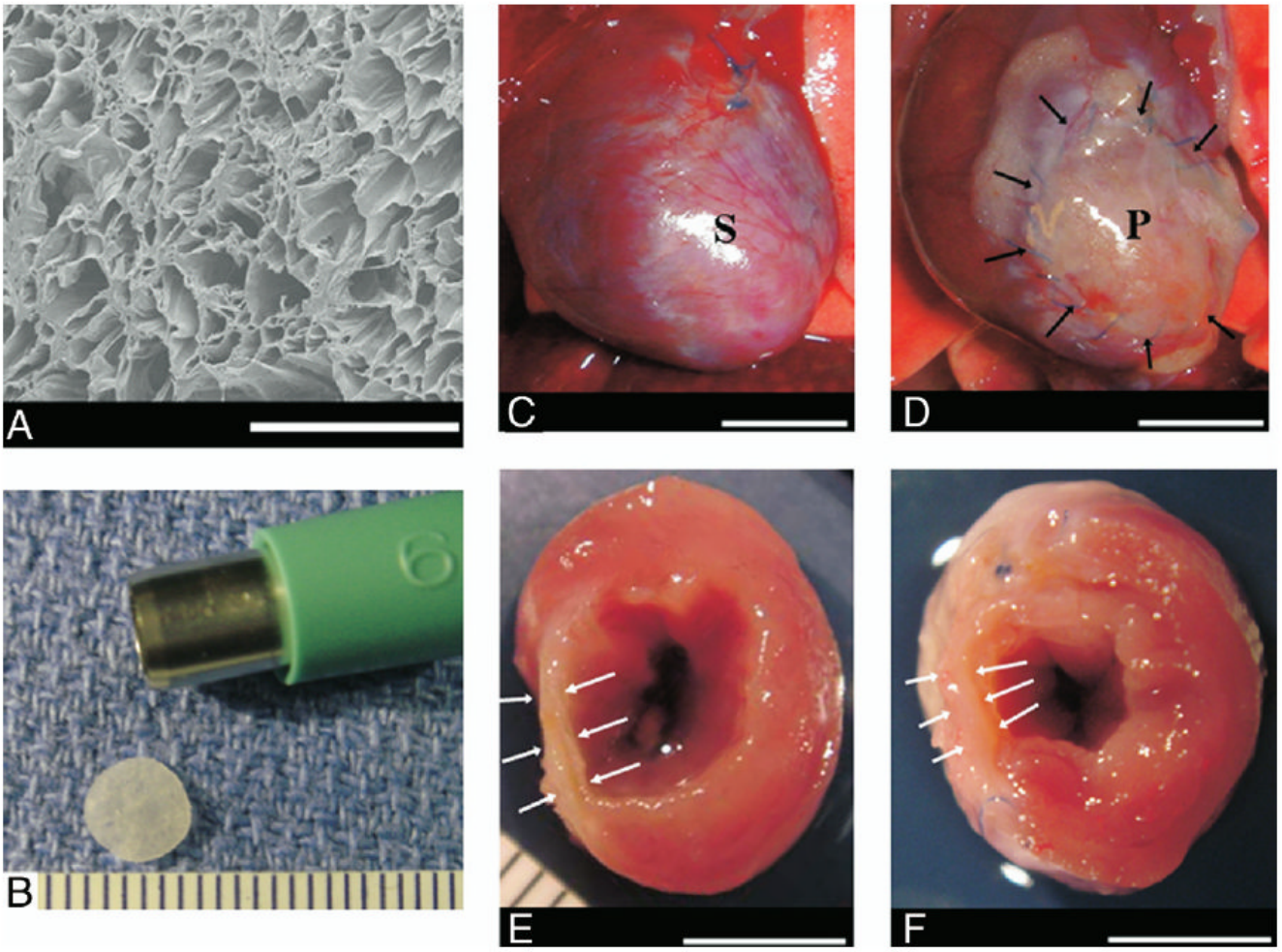

Figure 1. Features of PEUU and Representative Images, at 8 Weeks After Implantation

Electron micrograph of the polyester urethane urea (PEUU) material **(A)**. Polyester urethane urea patch in final format (6-mm diameter × 300 μm thick) **(B)**. Representative images, 8 weeks after implantation, of the anterior view of infarction control **(C)** and PEUU patched **(D)** hearts. The cross-sectional view of both groups is shown in **E** and **F**, respectively. **Black arrows** point to the implanted PEUU patch, and **white arrows** indicate the infarcted anterior wall. Scale bar: 500 μm in **A**, 1 mm in **B**, 55 mm in **C to F**. P = the patch implanted area; S = the infarcted scar.

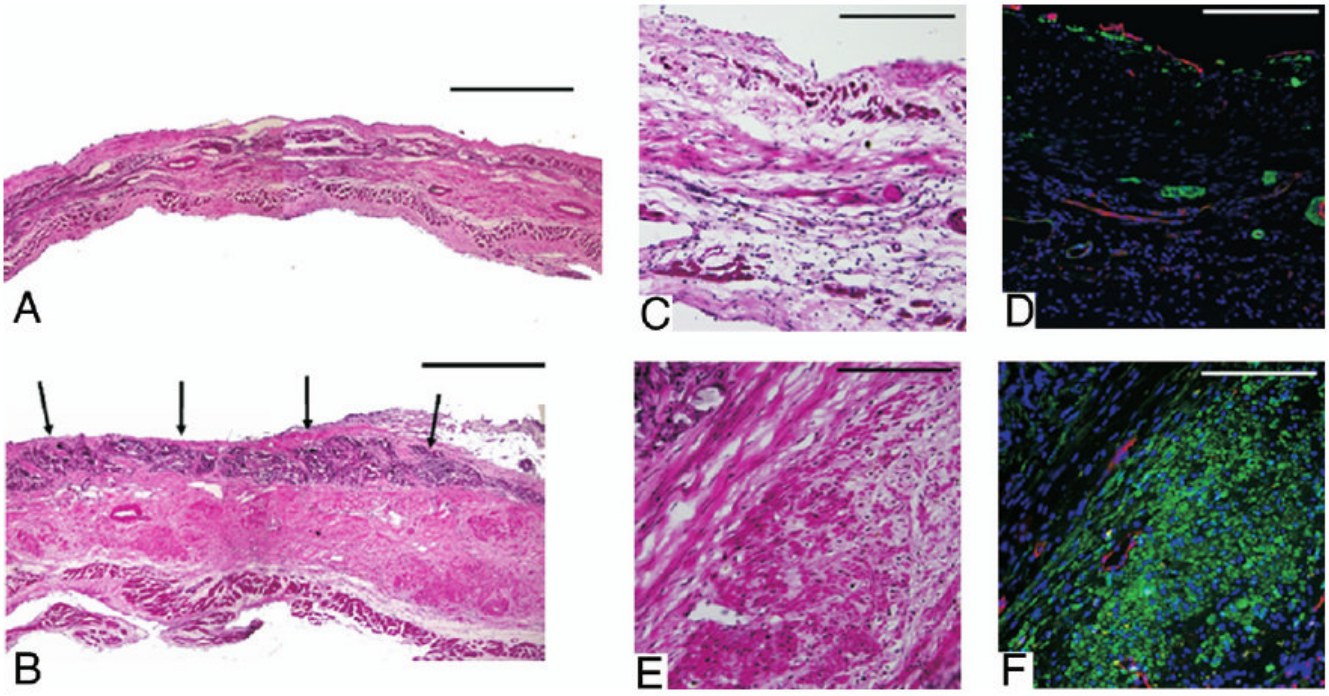

Figure 2. Representative Histological Sections

Representative histological sections of the infarction control **(A)** and PEUU patched **(B)** myocardial wall 8 weeks after implantation stained with hematoxylin and eosin. **Black arrows** indicate the top of the PEUU implanted area, which appears **dark violet**. Higher magnification of hematoxylin and eosin staining and immunohistochemical staining appear in **C to F** where **C** and **D** are infarcted control and **E** and **F** are PEUU patched. α-SMA staining appears **green**, CD31 staining appears **red**, and nuclear staining appears **blue**. Increased smooth muscle actin is apparent in the PEUU patched group. Scale bars in **A and B** are 500 μm. For **C to F**, scale bars are 200 μm.

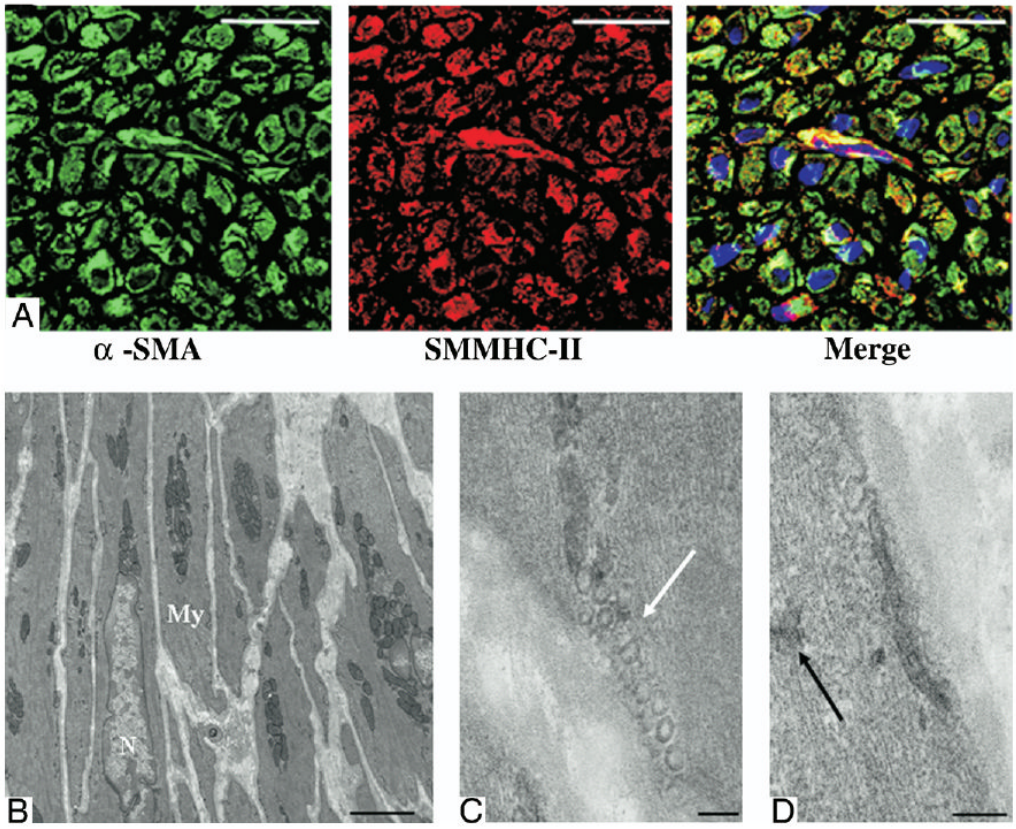

Figure 3. Characterization of *α*-SMA–Positive Cells

Smooth muscle myosin heavy chain isotype II (SMMHC-II) **(A)** immunohistochemical staining colocalized with alpha-smooth muscle actin (*α*-SMA)–positive cells suggesting mature contractile ability. Electron micrographs **(B to D)** of the muscle-like bundles beneath the polyester urethane urea patch exhibited ultrastructural features typical of mature contractile phenotype smooth muscle cells. **White arrow** denotes caveole. **Black arrow** indicates dense bodies. Scale bars for **A** are 20 *μ*m, for **B** are 2 *μ*m, and for **C and D** are 100 nm. My = myofibril; N = nuclear.

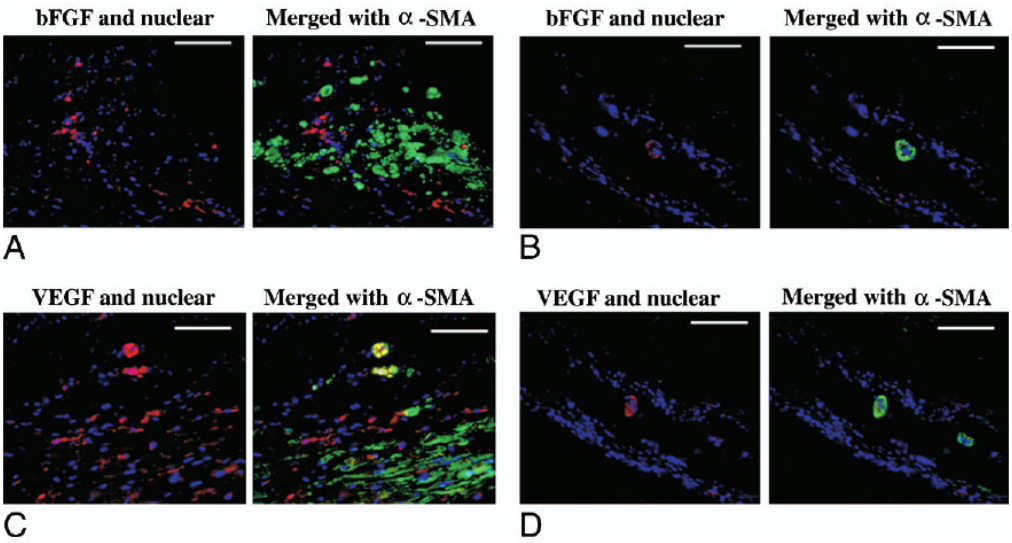

Figure 4. bFGF and VEGF Immunohistochemical Staining

Immunohistochemical staining for basic fibroblast growth factor (bFGF) **(A and B)** and vascular endothelial growth factor (VEGF) **(C and D)** in the polyester urethane urea patch **(A and C)** and infarction control **(B and D)** groups. The **left image of each set** shows growth factor and nuclear staining, and the **right image** merges in alpha-smooth muscle actin (α-SMA) staining. Growth factor staining is **red**, α-SMA staining is **green**, and nuclear staining is **blue**. Scale bars are 100 μm.

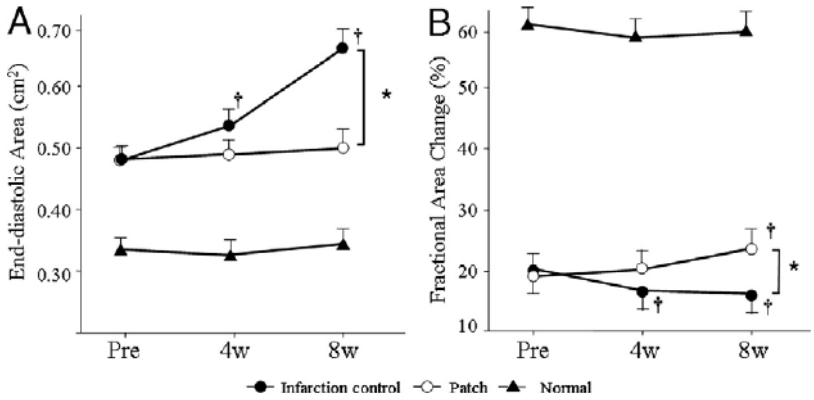

Figure 5. Echocardiographic Assessment

Echocardiographic assessment of the polyester urethane urea patch, infarction control, and normal control groups during the study period. End-diastolic area is shown in **(A)**, and % fractional area change in **(B)**. End-diastolic area and % fractional area change in the normal control group were significantly different than those in the patch and infarction control groups ($p < 0.05$) at each time point and did not significantly vary during follow-up. *$p < 0.05$ between groups; †$p < 0.05$ versus just before implantation (pre) within group. 4w = 4 weeks after implantation; 8w = 8 weeks after implantation.

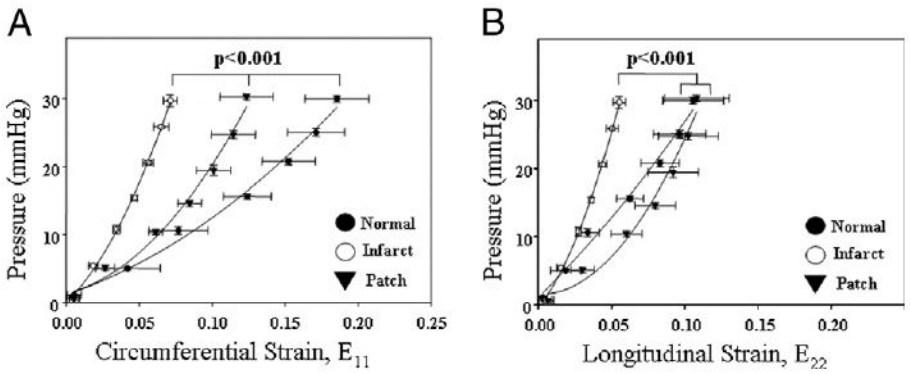

Figure 6. Pressure-Strain Relationship for Biomechanical Compliance

Pressure-strain relationship for biomechanical compliance of the left ventricular anterior wall. Circumferential strain (E_{11}) is shown in **(A)** and longitudinal strain (E_{22}) in **(B)**. For both directions, the infarction control group exhibited the least compliance, while the polyester urethane urea patch group was significantly more compliant, being between infarcted and normal or equivalent to normal tissue.